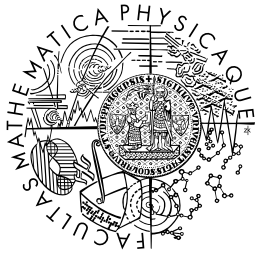

FACULTY
OF MATHEMATICS
AND PHYSICS
Charles University

BACHELOR THESIS

Ondřej Theiner

Tests of Semiconductor Detectors for ATLAS Upgrade

Institute of Particle and Nuclear Physics

Supervisor of the bachelor thesis:	RNDr. Peter Kodyš, CSc.
Study programme:	Physics
Study branch:	General Physics

Prague 2017

I declare that I carried out this bachelor thesis independently, and only with the cited sources, literature and other professional sources.

I understand that my work relates to the rights and obligations under the Act No. 121/2000 Sb., the Copyright Act, as amended, in particular the fact that the Charles University has the right to conclude a license agreement on the use of this work as a school work pursuant to Section 60 subsection 1 of the Copyright Act.

In Prague, 15 May 2017 Ondřej Theiner

Title: Tests of Semiconductor Detectors for ATLAS Upgrade

Author: Ondřej Theiner

Institute: Institute of Particle and Nuclear Physics

Supervisor: RNDr. Peter Kodyš, CSc., Institute of Particle and Nuclear Physics

Abstract: Together with the planned upgrade of the Large Hadron Collider at CERN, a lot of experiments on the LHC will have to be improved as well. This is also the case of the ATLAS experiment. This thesis focuses on laser testing of silicon strip detectors which will be part of the Inner Tracker in the improved ATLAS Upgrade experiment. The first two parts of the thesis describe the ATLAS Upgrade experiment and summarise the basic theory behind silicon strip detectors. The third and the main part of the thesis is dedicated to experimental part of my work, which consisted of the actual laser testing of silicon strip detectors. The fourth chapter discusses the results of my measurements. All the tests presented in this thesis were performed in the laboratory of the Institute of Particle and Nuclear Physics in Prague. Besides having performed the measurements of detection properties of strip detectors, several ROOT macros for automatization of these measurements were written.

Keywords: ATLAS Upgrade, laser testing, silicon strip detectors

Název práce: Testování polovodičových detektorů pro ATLAS Upgrade

Autor: Ondřej Theiner

Ústav: Ústav částicové a jaderné fyziky

Vedoucí bakalářské práce: RNDr. Peter Kodyš, CSc., Ústav částicové a jaderné fyziky

Abstrakt: Spolu s plánovaným vylepšením Velkého hadronového urychlovače LHC v CERNu bude muset být zdokonaleno i mnoho experimentů, které se na tomto urychlovači nacházejí. To je také případ experimentu ATLAS. Tato práce se zabývá testováním křemíkových stripových detektorů, které by měly být umístěny ve vylepšené verzi experimentu ATLAS Upgrade, pomocí laseru. První dvě části práce pojednávají o experimentu ATLAS Upgrade a shrnují základní teoretické poznatky o křemíkových stripových detektorech. Třetí a zároveň hlavní kapitola práce je věnovaná experimentální části, která se týkala samotného testování detektorů pomocí laseru. Čtvrtá kapitola diskutuje výsledky měření. Veškeré testy byly prováděny v laboratořích Ústavu částicové a jaderné fyziky v Praze. Kromě samotných měření bylo, za účelem automatizace těchto měření, napsáno několik maker využívající prostředí ROOT.

Klíčová slova: ATLAS Upgrade, laser testy, křemíkové stripové detektory

I would like to say thanks to my supervisor RNDr. Peter Kodyš, CSc. for being always willing to help me in solving issues with laboratory equipment and also for valuable pieces of advice about the thesis.

I am also very thankful to Jakub Vošmera for grammatical and typographical corrections.

Finally I am grateful to my family for supporting me in everything I do.

Contents

Introduction

It has been almost 2500 years since Democritus in ancient Greece first proposed idea that matter is composed of elementary, further indivisible, building bricks which he called atoms. He believed that structure of matter reflects the shape and the size of atoms it consists of. If we consider the era from which this hypothesis comes from we have to admire that he was not that far from what we know today, compared to other theories comming from these times.

But many years passed and our knowledge is further. We know that atoms are not indivisible but they consists of electron shell and nucleus, which further consists of protons and neutrons which themselves are made of quarks and gluons. We also know that there is many more elementary particles than people thought some 100 years ago and in a desire of describing them we are developing new physical theories.

All these things would not be possible without laboratories and experiments around the world. One example of such a laboratory is CERN[1] which is operating the largest particle physics laboratory in the world. Apart from a number of other scientific facilities there is also the world's largest and most powerful particle collider LHC[2] - a toroidal ring 27 km in circumference - running four main experiments: ATLAS, ALICE, CMS an LHCb. The goal of these experiments is to answer some fundamental questions about the constituents of universe and also to uncover hints of new physics which is beyond our current knowledge.

As a hunt for new physics goes on, all the experiments need to be upgraded from time to time to be able to fulfil the very high requirements which are being put on them. But currently this is the case of whole LHC, which should, in a future, be able to collide particles with higher integrated luminosity[3]. Consequently, an upgrade will be needed for many of the individual LHC experiments.

The ATLAS experiment is not an exception, especially its inner part which lies in the closest proximity of collisions. This thesis is dedicated to testing of silicon strip detectors by laser with all the measurements having been performed in the laboratories of the Institute of Particle and Nuclear Physics in Prague. These detectors will be placed in the upgraded version of the ATLAS experiment.

The thesis is divided into four chapters. The first chapter briefly describes the present ATLAS experiment and its upgraded version ATLAS Upgrade, with main focus on changes between these two versions. In the second chapter some basic principles of silicon strip detectors will be explained. The third, main chapter, will bring the reader closer to the experimental part of this thesis. Also the results of all the measurement performed are presented in this chapter. The last chapter contains discussion of the data aquired in these measurements.

The last two chapters represent work done mainly by the author. It can be summrised as a substantial contribution to setting up a source test system, performing measurements with a laser, contribution to data analysis, measurements

[1] Acronym of French words *"Conseil Européen pour la Recherche Nucléaire"* which means European Council for Nuclear Research.

[2] LHC is an abbreviation for Large Hadron Collider

[3] Luminosity is defined as a ratio of events detected in certain time per scattering cross-section. It is usually given in $\mathrm{cm}^{-2} \cdot \mathrm{s}^{-1}$. Integrted luminosity is defined as the integral of luminosity with respect to time.

of laser stability and interpretation of the results.

1. ATLAS Upgrade

Large Hadron Collider is the largest particle accelerator in the world situated at Swiss-French borders at CERN. It is a toroidal ring with circumference of 27 km equipped with superconductive magnets and other mechanisms which aim to accelerate particles, keep them on desired trajectories and then collide them inside one of the experiments. There are four main experiments along this toroidal tube. They are ATLAS, CMS, ALICE and LHCb. This thesis is related to the first mentioned one - experiment ATLAS.

The name ATLAS is an abbreviation of words "A Toroidal LHC Apparatus" and together with CMS it is the biggest experiment on LHC. It focuses on questions like what the matter consists of, why there is more matter in the Universe than antimatter as well as on some fundamental questions related to the Standard Model [1]. It is also the experiment where the Higgs boson was discovered.

But as the physics and technology is moving forward, requirements on LHC grow higher. Due to this fact, the High-Luminosity Large Hadron Collider (HL-LHC) project was initiated aiming to crank up the performance of the LHC in order to increase the potential for discoveries after 2025. The objective is to increase luminosity by a factor of 10 beyond the LHC's design value which is about $10^{34}\mathrm{cm}^{-2}\cdot\mathrm{s}^{-1}$ [2]. For this reason current experiments need to be upgraded as well.

ATLAS Upgrade is the new name for the improved ATLAS experiment. This improvement means that some parts of detectors have to be replaced by new components so that they satisfy new requirements enabling them to operate at higher luminosity. Institute of Particle and Nuclear Physics (IPNP) is one of the organisations participating on this upgrade. In particular, new silicon detectors, which should replace the present ones, are tested there.

1.1 Parts of the experiment

Upgraded ATLAS experiment will be, as well as the present ATLAS experiment, a very complex device because it needs to gather all the important information about collisions. And because there is about 600 millions inelastic proton-proton collisions per second, the whole experiment has to be designed so that it is capable of processing all the necessary information about collisions very fast. In the following sections, main parts of the future upgraded ATLAS experiment will be described. Schematics of the present ATLAS experiment is depicted on figure 1.1.

1.1.1 Inner Tracker

Currently the innermost part of ATLAS is called Inner Detector. It is the part of the experiment which is situated in the closest proximity of the tube where accelerated particles collide so it is also the first part of ATLAS to detect the decay products of collisions. The Inner Detector measures the direction, momentum and charge of electrically charged particles produced in each collision [4]. In its present state, the Inner Detector consists of three main parts which are - Pixel Detector,

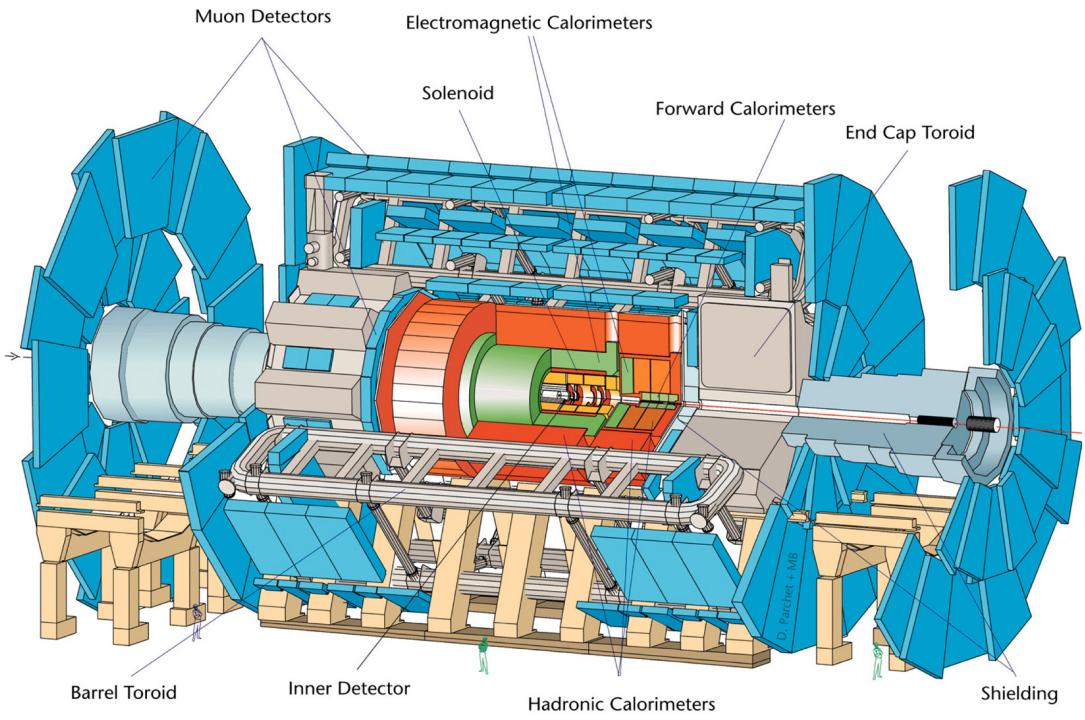

Figure 1.1: Schematics of the present ATLAS experiment. [3]

Semiconductor Detector (SCT) and Transition Radiation Tracker (TRT). After the upgrade, the Inner Detector will be completely replaced by the new Inner Tracker (ITk). Design of the ITk takes advantage of new technology developed since the construction of the existing Inner Detector: its performance will be enhanced by a lower mass construction, reducing the effect of multiple scattering, photon conversions and hadronic interactions. [5]

New Inner Tracker will be an all-silicon detector consisting of pixel and strip layers. Pixel and strip detectors will be placed around the locus of collision in the so called barrel and endcap[4] parts of the detector in several layers [5]. Figure 1.2 shows two possible layouts of strip and pixel detectors which were discussed when designing ITk.

1.1.2 Calorimeter

Calorimeter is a part of the experiment which is used to measure energy of particles coming from a collision. The present ATLAS detector system has two main components: Tile Calorimeter (TileCal) and Liquid Argon Calorimeter (LAr).

TileCal, 5.6 m long barrel with endcaps [7], consists of steel absorbers and active scintillation layers from which light signal is lead by optical fibers to photomultipliers. Energy of the original particle can be determined from this signal.

LAr is 6.4 m long barrel with endcaps. Those endcaps consist of the Forward Calorimeter and Electromagnetic and Hadronic Endcaps [7].

In contrast to the ITk, not all the parts of the ATLAS calorimeters will have

[4]Barrel is a part of ITk surrounding the pipe of the accelerator like a side of a cylinder whereas the endcap parts create bases of that cylinder.

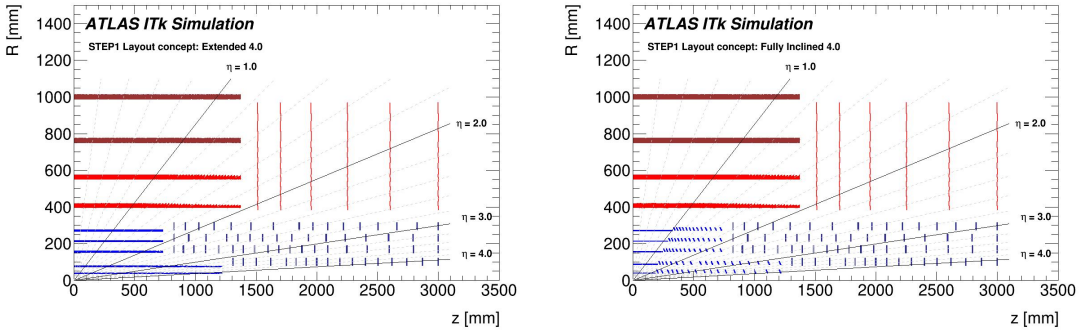

Figure 1.2: Figure showing two possible layouts of ITk Strip (light and dark red) and Pixel (blue) detectors layout. The diagram on the left depicts a layout where inner barrel layers are extended whereas the diagram on the right figure shows a situation where inner and outer parts of barrel are inclined. Simulations showed the second layout, where inner and outer parts of barrel are inclined, to be better which means, that this layout will be used in ATLAS Upgrade. Adapted from [6].

to be replaced in order to satisfy the requirements of HL-LHC. LAr Electromagnetic Calorimeters, TileCal and Hadronic Endcap Calorimeter currently maintain required performance under HL-LHC so they will stay the same even in ATLAS Upgrade. On the other hand, the LAr Forward Calorimeters will have to be replaced because they would be degraded by high energies and particle densities in HL-LHC. Also, new High Granularity Timing Detector will be installed in front of LAr Calorimeter endcaps [5].

1.1.3 Muon Spectrometer

Muon Spectrometer (MS) is a detector which measures momenta of muons. These are particles that cannot be detected by ITk or Calorimeter. MS consists of of three large air-core superconducting toroidal magnet systems[5]. Deflection of muon trajectories is measured by hits in tree layers of precision drift tube chambers and cathode strip chambers. There are also three layers of resistive plate chambers in a barrel part of MS and three layers of thin gap chambers in endcaps which provide a muon trigger and also measure muon trajectory in a plane in which it is not bent by magnetic field. New MS should be able to detect muons with higher pseudorapidity[6] (up to $\mid \eta \mid = 4$). For ATLAS Upgrade, some parts of endcap layers will have to be replaced.

Currently, ATLAS detector MS also provides a level-1 hardware muon trigger. After a muon is detected by the level-1 trigger, high-level trigger confirms or denies measurement using data from precision chambers. Present trigger system would not be able to cope with the HL-LHC requirements which means that some changes to the trigger system of MS will have to be made.

Readout electronics of several parts of MS will also have to be improved so as to be able to cope with higher trigger rate in the HL-LHC enviroment [5].

[5] with two endcaps and one barrel

[6] Pseudorapidity η is a spatial coordinate used in particle physics which measures the angle between particle three-momentum and the beam axis. It is defined as $\eta \equiv -\ln\left[\tan\left(\frac{\theta}{2}\right)\right]$ [8].

1.1.4 Trigger and Data Acquisition System

Up to one billion proton-proton collisions per second can occur in the present LHC setup. If we wanted to store information about all collisions, we would have to store approximately 60 terabytes of data per second. This would be barely possible to process. However, if we asume that not all the events are interesting for us, the task becomes more realistic. For that reason, ATLAS is equipped by the Trigger and Data Acquisition System (TDAQ) which filters out most of the unimportant data and stores only those which might be potentially interesting.

ATLAS's trigger system has three levels. Level-1 trigger works only on a subset of data from the calorimeter and the muon detector. It decides whether to keep or discard the event in just a few μs. As a result, out of circa $4 \cdot 10^7$ bunchcrossings per second, less than 10^5 are kept by this trigger.

Data which pass through Level-1 trigger proceed to the Level-2 trigger. The Level-2 trigger is a large array of processors analysing data in a greater detail.

Only a few thousand events per second are selected by Level-2 trigger and go to Level-3 trigger which is a farm of CPUs inspecting the data into a deeper detail. Finally about 200 events per second are left and stored for a later offline analysis [9].

Facts stated above for TDAQ apply to the present ATLAS experiment. If we assume a higher collision rate for the ATLAS Upgrade, it is evident that the current TDAQ system will have to be modified to be able to cope with the HL-LHC environment.

1.1.5 Magnet System

A system of magnets bends particles tracks, thus allowing the scientists to determine the charge and momentum of these particles. ATLAS's magnet system contains three main components: Central Solenoid Magnet, Barrel Toroid and End-cap Toroids. The Barrel Toroid covers the central region, whereas forward regions are covered by two End-cap Toroids. Magnetic field in the central tracking volume is provided by the Central Solenoid [10]. The whole system is designated to provide a stable, precise and predictable magnetic field in an enormous volume.

2. Semiconductor detectors

2.1 Basic principles

In order to be able to detect products of a collision in a particle physics experiment, we need a device which is capable of detecting those products - a detector. There are many types of detectors. In this section we will focus on position sensitive detectors with special emphasis on semiconductor detectors.

Semiconductors are elements of the IV.A group in the periodic table which means that if they are arranged in a lattice, they share four valence electrons with the neighbouring atoms. They can be divided into several groups. One possible division is into intrinsic and extrinsic semiconductors. Intrinsic semiconductors contain only atoms of one type whereas extrinsic semiconductors contain a dash of atoms of different type. Extrinsic semiconductors can be further divided into p and n-type semiconductors depending on type of atoms added.

If we add atoms with three valence electrons (e.g. boron) we get a p-type semiconductor. Three valence electrons of the added atom cause a vacancy of one electron in the valence band that can be easily occupied by another electron which leads to a movement of the vacancy and thus transport of electric charge.

We can also add atoms with five valence electrons (e.g. arsenic). If we do so, we get an n-type semiconductor. In this type of semiconductor, the fifth electron of an extrinsic element is very weekly bound to its original atom so it can easily transport electric charge.

The basic principle of semiconductor detectors is based on the properties of band structure of semiconductors. Semiconductors are materials with a thin gap between the valence and the conduction band. This means that a little amount of energy is necessary to get an electron from the valence band to the conduction band. The width of the gap between the bands depends on the particular type of semiconductor. If a semiconductor detector is hit by a particle with energy higher than the width of the gap, an electron from the valence band can go to the conduction band. In addition, if an external electromagnetic field is present, electric current inside the detector starts flowing. This current can later be detected.

An advantage of semiconductors over other detection media is their thin gap between the valence and the conduction band which allows us to detect less energetic particles in comparison for example with gaseous ionization detectors. Other advantages of semiconductors used as detectors are their high density leading to a high ionizing energy loss, their mechanical strength and also high mobility of charge carriers [11].

2.1.1 *p-n* junction

Probably the most important part of a semiconductor detector is the p-n junction. p-n junction is an interface between the p and n-type semiconductor. Putting p and n-type semiconductors together causes that electrons move to p region whereas vacancies move to the n region of a junction. This leads to creation of electric field.

The main feature of p-n junctions is that it can conduct electric current only

if it is put into electric circuit in the so called forward direction. If we put it into electric circuit in the reverse direction, it leads to creation of depleted area in a region around the junction and positive and negative charges on the edges. Now if a particle passes through the junction, it excites atoms in the depleted area. Hence, the originally neutral depleted area will now be endowed with charge which, in case that an external electric field is present, will cause detectable flow of electric current.

2.2 Strip detectors

We can distinguish several types of position sensitive semiconductor detectors but because the experimental part of the thesis focuses solely on silicon strip detectors, only this type of detector will be discussed.

The name of this type of detectors is derived from the shape of electrodes collecting electric charge. Electrodes have a thin strip-like shape and are arranged in parallel to each other. In the case of the detectors tested within this thesis, a typical width of strips was about $25\,\mu$m and the pitch of strips was $80\,\mu$m[7].

The position of a spot where a particle hits the detector is then determined based on which strip collected the charge generated in the semiconductor by particle flyby. Due to geometry of the electrodes (parallel strips) only the coordinate perpendicular to strips can be determined.

There are other types of semiconductor position sensitive detectors (e.g. pixel detectors) but as they are not subject of this thesis they will not be discussed more.

2.3 Detector readout

We can distinguish between two types of detector readout. The first type is analog readout. It gives us information about amplitude of signal[8] from a detector. On the contrary the second type, which is binary readout, gives us only logical (binary) information whether the signal we detect is higher or lower than present threshold.

The second type is the one which is used in current ATLAS experiment in the Inner Detector (will also be used in ATLAS Upgrade in Inner Tracker) and it is therefore used by detectors tested within this thesis. The reason for usage of binary readout is the data amount reduction. These detectors are used for particle tracking in which we need to know where the particle went and so we do not need information about amplitude. But for detector testing it is desirable to have information about charge generated in silicon part of a detector. Even though we use binary readout, it is still possible to determine the amount of generated charge. Or to be more precise, we are not able to estimate an amount of a charge generated by a single particle but we can determine an average amount of charge generated by particle flyby from set of trials. To do this, we have to

[7]Values listed here are the typical dimensions but it is important to say that these values can slightly vary (within several μm).

[8]Strength of signal is proportional to charge generated in silicon.

perform test called threshold scan, principle of which is explained in subsection 2.4.1.

2.4 Detector characterisation

2.4.1 Threshold scan

Threshold scan is a basic test in which we detect relation between number of detected hits from set of trials[9] and threshold. The value of the threshold is in the case of tested detectors given in the internal units of the analog-to-digital converter called DAQ counts. These units correspond to voltage detected on readout electrodes (strips) which can later be converted to charge[10]. If we had no noise, the result of this measurement would be step function as it is an integral of delta function signal. In fact, the real signal is a convolution of Landau distribution[11] and Gaussian distribution[12] which is sometimes called Langaus distribution. This Langaus widening causes that the result of a threshold scan is, instead of step function, skewed complementary error function which is defined as

$$f(x) = \epsilon_{max}\text{erfc}\left[x\left(1 + 0.6\frac{e^{-\xi x} - e^{\xi x}}{e^{-\xi x} + e^{\xi x}}\right)\right] \tag{2.1}$$

where erfc is the error function, ξ is a skew factor and ϵ_{max} is half of S-curve maximum.

If we fit the skewed complementary error function to the measured threshold scan data, we can directly obtain information about the noise (standard deviation) and the so called vt50, which is the value of threshold where signal drops to 50% (mean).

2.4.2 Strobe delay

If we want to know what the relation between the signal from the detector given in DAQ counts and the signal given in fC [13] is, it is necessary to perform a calibration procedure which uses an internal calibration pulse as described in the subsections below. To do this, we need to set the time delay between the calibration pulse and readout. Strobe delay is a procedure which finds the best timing between the calibration pulse and readout and sets this value to readout electronics.

2.4.3 Response curve

Response curve is a relation between signal from the detector given in mV and the information given in fC. This relation is obtained by measurements using

[9] During the tests discussed further in the text we detect a few ns lasting laser pulse with constant intensity.

[10] Typical thickness of silicon detectors tested within this thesis is about 300μm and so the charge generated in silicon by creation of electron-hole pairs is usually about few fC

[11] Typical character of energy distribution in matter from particle's flyby.

[12] Typical distribution of noise.

[13] Details of conversion between DAQ counts and fC will be explained in subsection 3.4.3.

an inner calibration pulse where we know the charge that we injected into the detector and the response we measure. A typical response curve is plotted on graph 2.1.

2.4.4 Three point gain

Measurement of the whole response curve may sometimes take an unnecessarily long time, especially if we do not need the whole response curve but only its initial part which behaves linearly. For this reason, we can measure the so called three point gain (3PG), which is a response curve measured in three points for charges where the behaviour is linear.

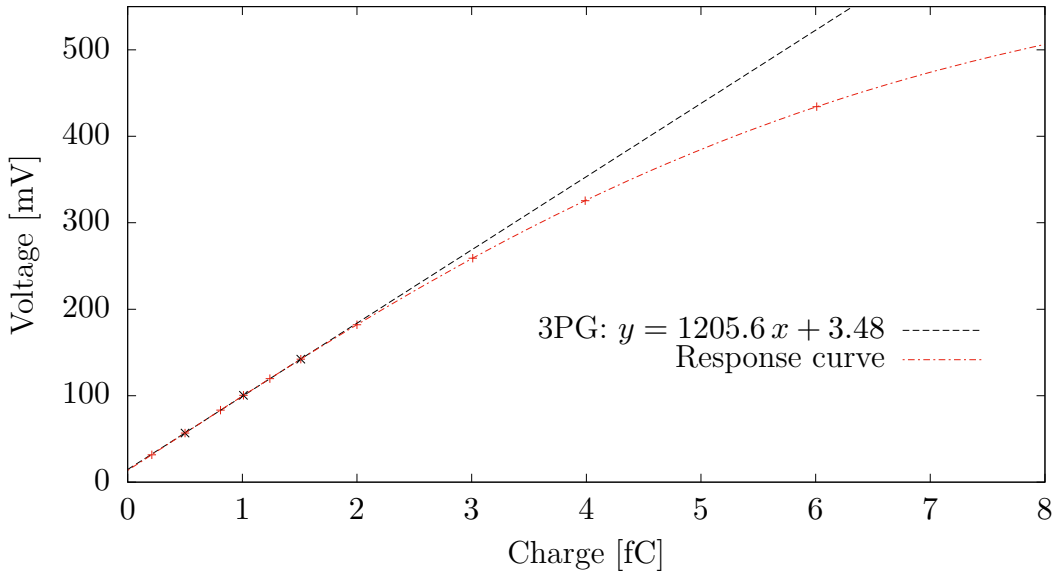

Graph 2.1: Response curve and three point gain.

3. Experimental part - laser tests

If we want to test detection properties of a silicon strip detector we have several options. The first one is to use radioactive source of β particles. Advantage of this test is that it is relatively cheap and can be done in a laboratory equipped for it. Disadvantage of this method is that we can not really focus β particles, meaning that we do not know their tracks.

However, there is a second method which is also quite accessible but allows us to hit specific part of the detector - this method is called laser testing. It is a general name for tests that use laser for detector illumination. Advantage of laser usage is that laser can be focused, thus enabling us to hit a specific part of the detector. Spot of a well focused laser on the detector is only few μm in diameter - distance which is much smaller than the gap between two strips.

The last method is test beam. It uses accelerated particles. On one hand, it best simulates the environment in a real LHC experiment, but on the other hand it is very expensive and not so accessible because it requires a particle accelerator. This is the reason why test beams are usually organised two or three times a year.

Experimental part of this thesis is about the second method mentioned above. All tests were performed on a newly created module which has not been tested as yet. Hence the results of this thesis can contribute to the further knowledge about the inspected silicon strip detectors.

3.1 Experimental setup

For all measurements performed within this thesis we used following experimental setup.

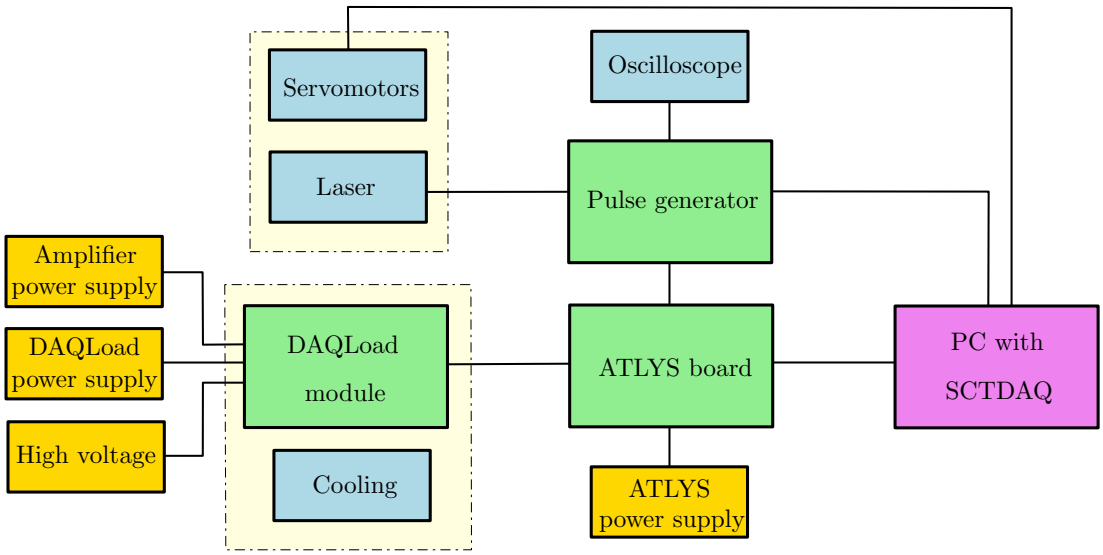

Figure 3.1: Scheme of experimental setup used for measurements.

It consists of four main parts, which are PC with SCTDAQ, DAQLoad module with strip detector, laser and ATLYS board.

PC is the part of the experiment where all measurements are controlled from and SCTADQ is a software used for acquisition, visualisation and analysis of

measured data. SCTDAQ also has predefined some useful standard tests like for example the threshold scan, which is the test we will use later.

Next part of the experimental setup is DAQLoad module with the silicon strip detector we are testing. This module is, apart from the detector itself, equipped with front-end electronics[14] which is necessary but it also can be a source of unwanted heat. In the case that chips on the module can not cool themselves, external cooling have to be applied. Whole module is closed in the so called black box, which is thermally isolated box with no external light access.

Because we are going to do laser tests, the third part of the setup is laser. We used infrared laser with wavelength of 1060 nm. The laser is fixed to positioning stages, which allow us to move the laser in three perpendicular directions with submicron precision. The laser is also connected to a pulse generator controlling the shape of the laser pulse. Positioning stages and pulse generator are, as all the other parts of the experiment, controlled via PC.

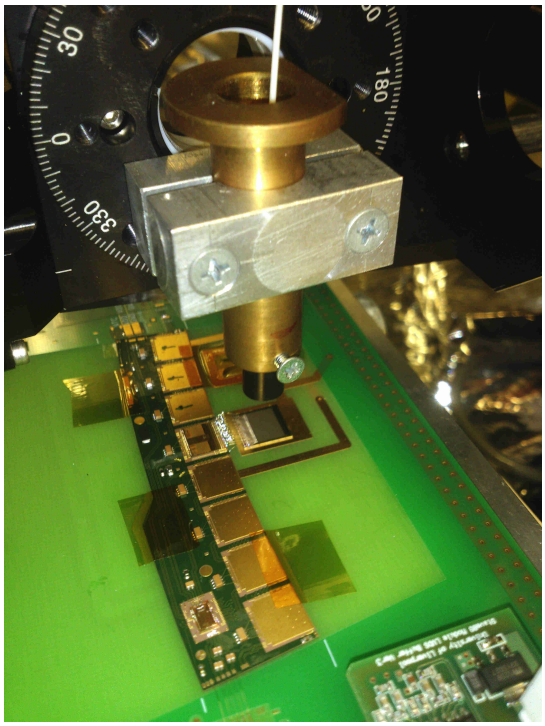

Figure 3.2: Detail of the tested module and laser attached to the moving stage. The laser beam is led by optical fibre above the detector where it is focused by the lens. The white optical fibre can be seen on the top of the figure, the lens is fixed at the bottom of the golden cylinder and the strip detector is the small shiny rectangle in the middle of the figure, just below the laser.

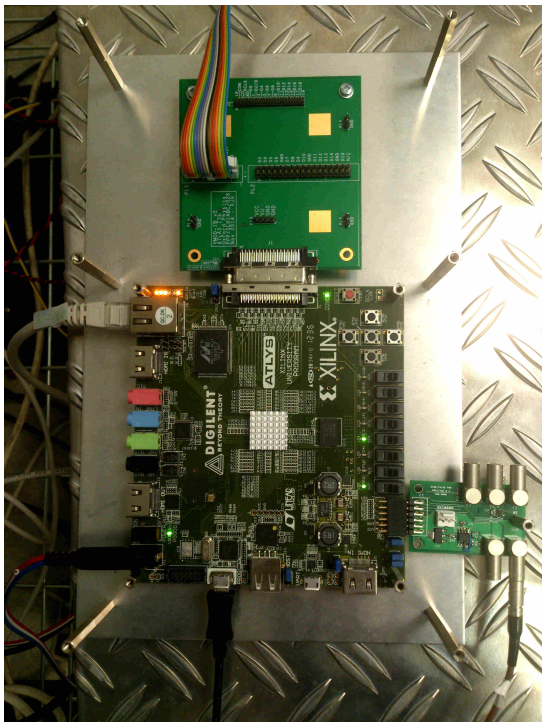

Figure 3.3: ATLYS board which intermediates communication between the DAQLoad module and the PC and also between the pulse generator and the detector.

[14] Front-end electronics is a term used for designation of electronics which provides detector readout and first signal processing on the most basic level. By this we mean, for instance, signal amplification or converting an analog signal to digital.

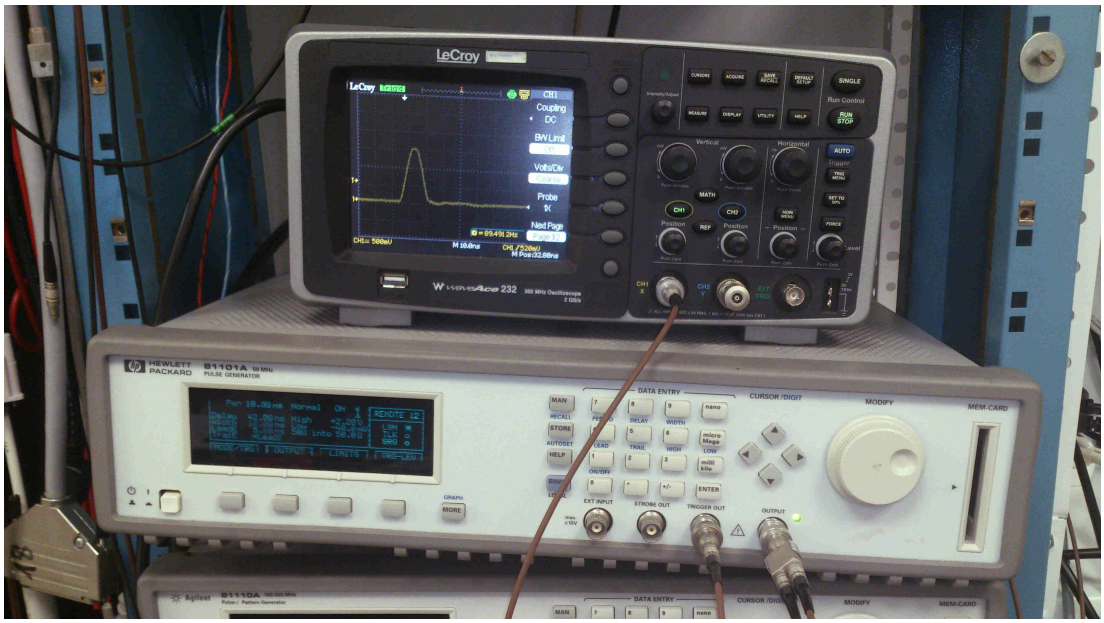

Figure 3.4: Pulse generator (white device) with an oscilloscope connected to it. The shape of a laser pulse can be seen on the screen of the oscilloscope.

Figure 3.5: A photography of the clean room where all tests were performed. The big white box on the right side of the picture is a black box. The two smaller boxes on it are the red and infrared lasers. Finally on the left side of the picture there are power supplies and pulse generator.

3.2 Laser focusing

In the following parts of the thesis, a cartesian coordinate system with following labelling of axes will be used. Axis perpendicular to the surface of the detector will be denoted z-axis, y-axis is parallel to the surface of the detector and perpendicular to strips direction and finally, x-axis will be parallel to both the surface of the detector and the direction of strips.

Before performing laser tests, it is important to have the laser well focused. Laser focusing means finding suitable distance between focusing lens and the detector so that focus of the lens lies on the detector. In the following paragraphs, the laser focusing procedure will be described. For this task, we will need the whole experimental setup working properly. Once we achieve this, we can open ATLAS SCTDAQ software on the computer which communicates with the tested module so that we can see the signal from individual strips in real time. After having all things prepared we can start focusing which can be divided into three steps.

Rough focusing

At first we may want to have the laser focused on the surface of the detector or under the surface depending on what we want to study. In the following paragraph, focusing on the surface will be described.

As the first step, we roughly have to find the place where the laser beam is focused. This is done by moving the laser in z-axis so we have response from a minimum number of strips. Close to this position, we find that if we move the laser up and down, the number of strips with response does not change. This is because of the shape of laser beam which passes through the lens. To find such a position, we move the laser in a direction in which we see the number of strips with response decreasing [15]. If we observe that the number of responding strips is minimal and does not change it means that the beam waist is close to the detector's surface[16]. Now we should slow down and keep moving the laser in the same direction until the number of responding strips increases again. If we find a position where we see an increase in the number of strips with response, we have to change the direction of our movement until we find second position in which the number of responding strips starts increasing again. The position that we are looking for is directly between these two positions.

If we wanted to focus the laser to a certain depth of the silicon detector (under the surface of the detector) we can do it in the following way. First we focus the laser on the surface of the detector by the method described in the paragraph above and the following two subsections. Then we move the laser closer to the surface so that the focus is in the required depth of silicon. Nevertheless it is necessary to keep in mind that we have to take into account the index of refraction of silicon[17], which causes that we have to move the laser in z-axis less than a depth of the layer we want to focus on.

[15] Initially we don't know where the focus is so we can be below or above the right position.

[16] We can also observe the signal to disappear completely. This could be caused by three factors - either we are too close or we are too far (laser spot is too large so that the intensity drops under detection limit) or we are directly pointing on a strip.

[17] Optically denser environment than air.

Finding the middle of a strip

If we focused the laser only in the way described in the previous paragraph, our focalization could have some flaws. The reason is that we do not know, where exactly the laser beam is pointing - whether it is directly between strips or whether the laser spot is hitting the strip only partially which can lead to unwanted reflection causing false signal on neighbouring strips. To avoid this effect, we have to find the middle of strip.

Finding the middle of strip is similar to finding the actual position of the z-axis position with the only difference that we are moving in the direction of y-axis. By moving the laser in y-axis we find two closest points in which we observe that the signal from the strip disappears and than reappears on the neighbouring strip. The position we are looking for again lies directly between these two. Having found the middle of strip we can proceed to the last step.

Fine focusing

This step is analogous to rough focusing described in the first part with the only difference being that now we should observe no response from the detector when the laser beam waist is close to the detector. By moving the laser in z-axis, we find two positions where the beam waist is under and above the surface of the detector when the signal first appears again. The final position of the laser is in the middle of these two positions.

Finally, it should be mentioned that we assumed the laser beam to be perpendicular to the detector. If it was not the case, this method would still work but the result would not be as good.

3.3 Tests with laser

3.3.1 Trigger delay scan

Before performing any laser tests, it is necessary to have the whole experimental setup well-set. Besides many things, like, for instance, having the laser focused, it is also important to maintain good timing between readout and laser pulses because this parameter directly influences the amount of signal we get from the detector. If the delay is not properly set, it can happen that we get no signal from the detector because the laser pulse comes after the detector readout[18]. To find a suitable timing, we measure relation between vt50 and time delay, which means we have to perform the threshold scan for each value of time delay of the laser pulse (trigger) and see when there is the best response from the detector.

The dependence was measured for two positions of the laser for channel number (strip) 474. During the first measurement, we placed the laser so that the response from one strip is the highest whereas during the second measurement the laser beam pointed near the strip. Results of these measurements are shown in graphs 3.1 and 3.2.

We can see three maxima and three minima in graphs. The reason we observe this effect is because of the way how we retrieve information from the detector.

[18]This parameter is analogous to strobe delay described in subsection 2.4.2

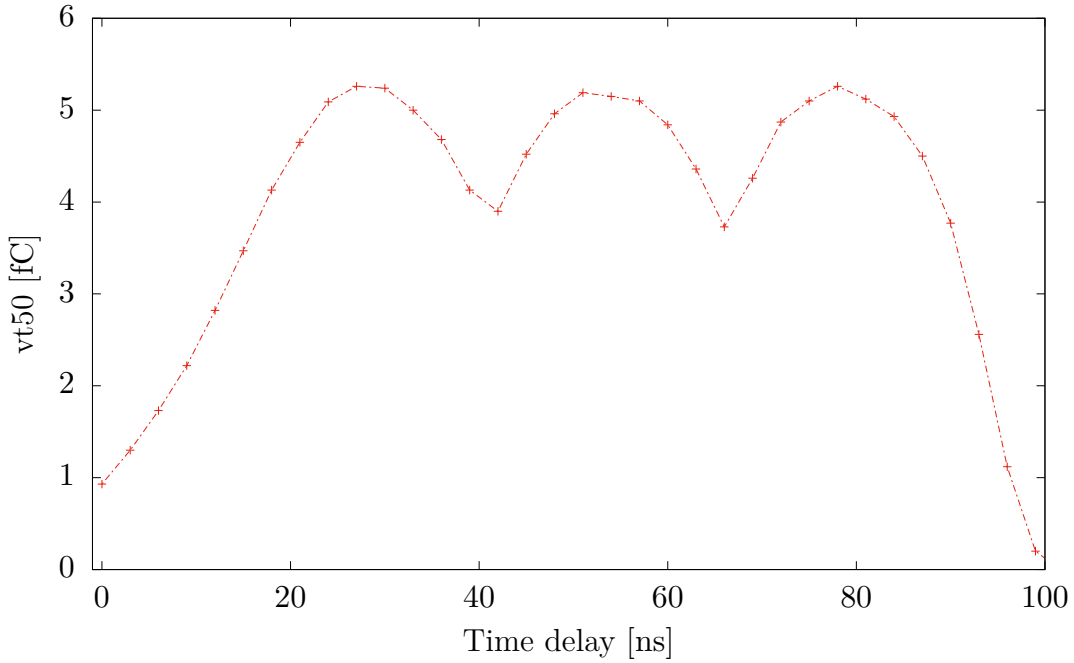

Graph 3.1: Dependence of vt50 on time delay of laser pulse. Laser beam hits the detector in a position where response from one strip is the highest (which is approximately 20 μm from the edge of strip). Uncertainty of data points is usually less than 2%. Points with vt50 lower than 0.1 fC may have uncertainty up to 3.5%. The values of uncertainties were estimated by SCTDAQ as the uncertainty of fit of skewed error function.

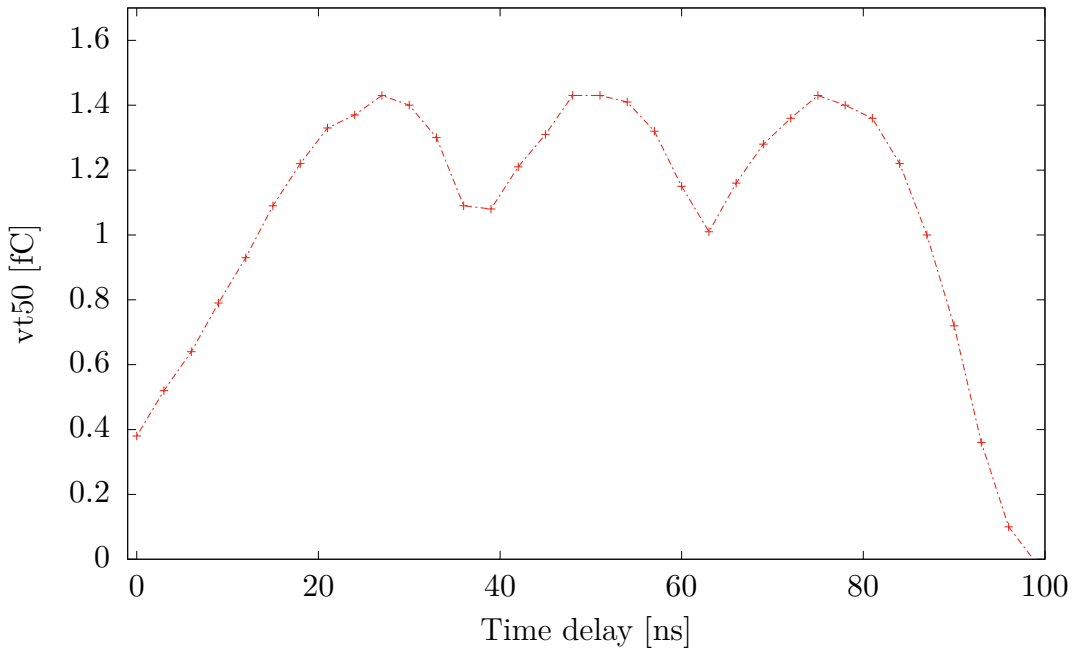

Graph 3.2: Dependence of vt50 on time delay of laser pulse. Laser beam hits the detector approximately 10 μm from from the edge of strip. Uncertainty of most of the points is less than 2%. Points with vt50 lower than 0.1 fC may have uncertainty up to 3.5%. The values of uncertainties were estimated by SCTDAQ as the uncertainty of fit of skewed error function.

Readout is performed every 25 ns which is exactly the time between the collisions of the bunches in LHC. One may notice that distance between maxima in the measured dependence is also approximately 25 ns. Explanation for these drops is that the charge generated by a laser pulse in silicon is not completely collected in one time bin and due to limitations of front-end electronics of the detector, signal loss occurs.

Also, note that we observe different scales on y-axis in the graph 3.1 and graph 3.2. The reason for this is the fact that because on graph 3.2 the laser beam partially hits metallic strip and so not all the light from the laser hits the silicon part of the detector where it creates charge.

Measurements were performed at temperature about 24.6 °C and pressure about 1020 hPa. Peak voltage of a pulse from pulse generator[19] was set to 2.15 V and the width of a pulse was set to minimal value allowed by the pulse generator which is 10 ns on pulse generator.

3.3.2 Dependence of standard deviation σ on trigger delay

Thanks to the measurements performed in the previous section, results of which are summarized in graphs 3.1 and 3.2, we know the dependence between trigger delay and vt50. However, one may be also interested in what the dependence of standard deviation σ from illuminated part of the detector vs. trigger delay looks like and how different sources of uncertainties contribute to this standard deviation. The following graphs 3.3 and 3.4 illustrate the relation between trigger delay and the relative standard deviation[20] of the signal from strip illuminated by laser. Method of separating the overall standard deviation into individual contributions is described in the following subsubsection.

If we compare the results presented in graphs 3.3 and 3.2 with the results displayed in graphs 3.1 and 3.2 we can notice that the relative standard deviation increases when signal from the detector is weaker. This is because of decreasing the signal-to-noise ratio.

Second thing which can be read from graphs 3.3 and 3.4 is that the biggest contribution comes from the laser and contributions from the strip and front-end electronics are approximately equal.

Obtaining individual contributions to σ_{total}

First, it is important to realise how and when particular components, i.e. laser, strip and front-end electronics contribute. A strip which is illuminated by the laser is obviously affected by all sources of noise: laser, strip and front-end electronics. On the other hand, the strips which are not illuminated are not affected by the laser. These two pieces of information are enough to reconstruct the contribution from the laser. If we denote by σ_{total} the overall contribution to standard deviation from an illuminated strip and by $\sigma_{\text{FE+strip}}$ the overall contribution from

[19] On pulse generator this parameter is called "High".

[20] Relative standard deviation is calculated as $\frac{\sigma}{\text{signal}}$, where signal is vt50 from the strip illuminated by laser.

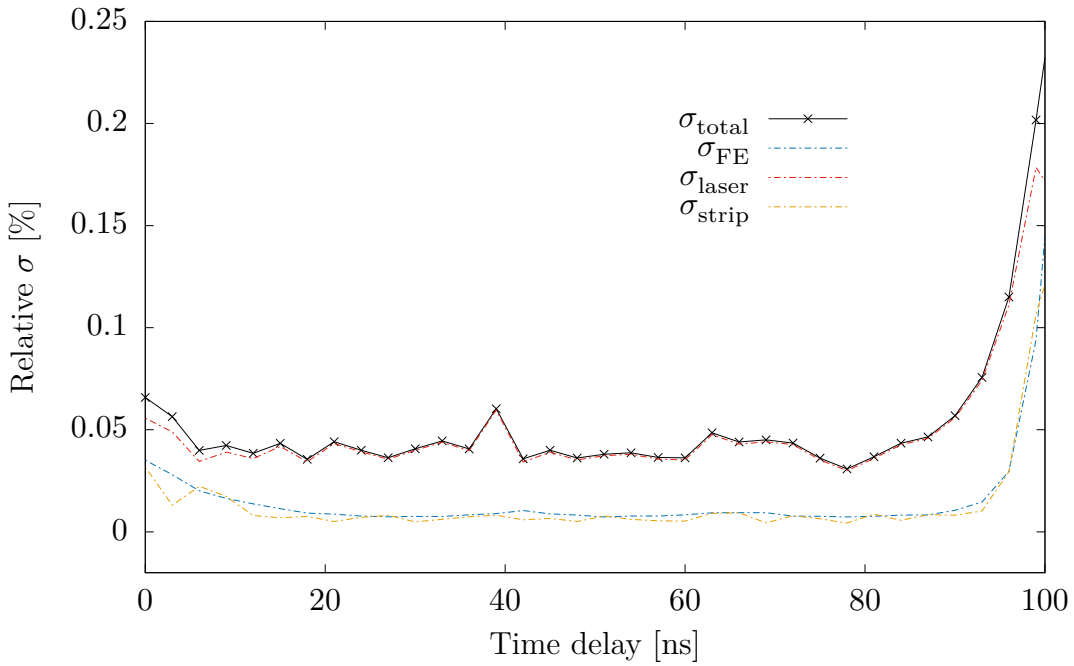

Graph 3.3: Dependence of overall relative standard deviation σ_{total} of S-curve, obtained from threshold scan, on the delay of laser pulse (trigger). The laser was located at the same position as in the case of graph 3.1. Overall σ_{total} was separated into contributions from the laser σ_{laser}, front-end electronics σ_{FE} and strip σ_{strip}. Uncertainty of σ_{total} is about 20% which is the value estimated by SCTDAQ.

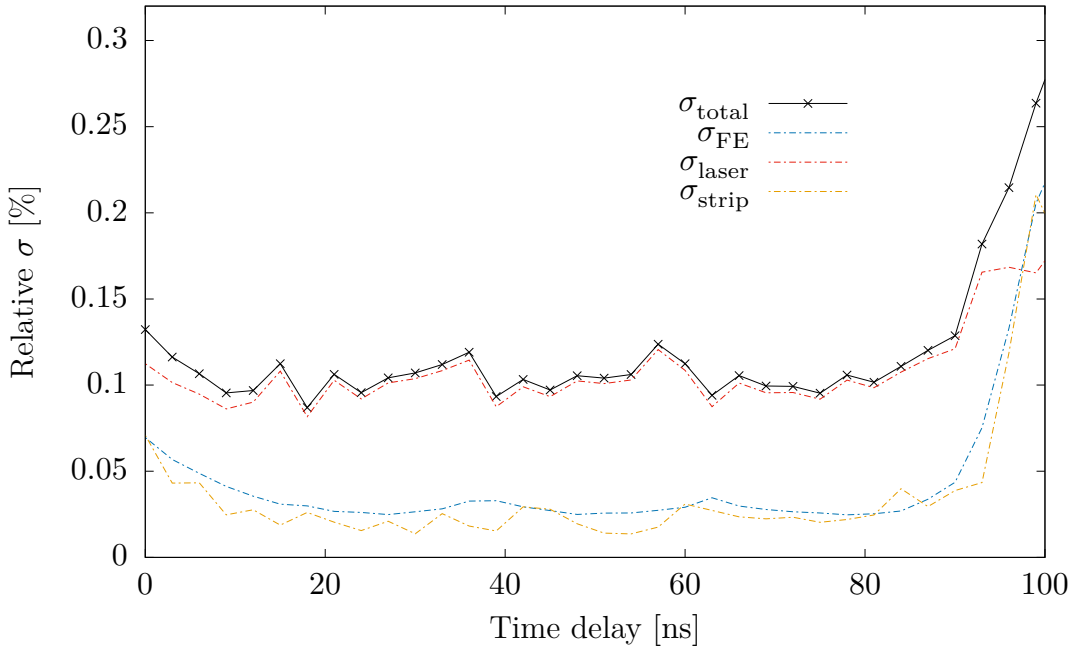

Graph 3.4: Dependency of overall relative standard deviation σ_{total} of S-curve obtained from threshold scan on the delay of laser pulse (trigger). The laser was located at the same position as in the case of graph 3.2. Overall σ_{total} was separated into contributions from laser σ_{laser}, front-end electronics σ_{FE} and strip σ_{strip}. Uncertainty of σ_{total} is about 20% which is the value estimated by SCTDAQ.

a strip which is not illuminated by the laser[21], we have for σ_{laser}

$$\begin{aligned} \sigma^2_{\text{total}} &= \sigma^2_{\text{FE+strip}} + \sigma^2_{\text{laser}} \\ \sigma_{\text{laser}} &= \sqrt{\sigma^2_{\text{total}} - \sigma^2_{\text{FE+strip}}} \end{aligned} \tag{3.1}$$

However, this information is still not enough to reconstruct contributions from the front-end electronics and the strip. To do this, further information is needed. This information can be obtained from the second row of strips which are not bonded[22]. Because they are not bonded the only source of errors that has to be taken into account is front-end electronics. So σ_{FE} is directly taken as an average value of standard deviation from these strips. Now we can separate σ_{strip} and σ_{FE} thanks to the relation

$$\begin{aligned} \sigma^2_{FE+strip} &= \sigma^2_{\text{strip}} + \sigma^2_{\text{FE}} \\ \sigma_{\text{strip}} &= \sqrt{\sigma^2_{FE+strip} - \sigma^2_{\text{FE}}} \end{aligned} \tag{3.2}$$

3.3.3 Interstrip scan

Interstrip scan is a type of measurement where we study the relation between the response of a detector (vt50) and position of the laser beam. This measurement is an important test of a detector, thanks to which we can decide if a detector behaves as we expect. The kind of behaviour we would like to see is that all the charge generated by a particle hitting the detector is collected, no matter which part of the detector was hit[23]. This requirement seems obvious but it might happen that it is not fulfilled[24].

Results of this measurement are shown in graph 3.5. This scan covered 200 μm so we can see the response from four neighbouring strips and also the sum of signal from all these four strips.

3.3.4 Two-dimensional scan

To visualise the relation between laser position, trigger delay and vt50, we can make two-dimensional scan. It means running the trigger delay scan for each laser position so that we obtain a two-dimensional matrix of vt50 values where the first coordinate is laser position and the second is trigger delay. The advantage of this kind of measurement is that we obtain complete information about relation between laser position and trigger delay. Disadvantage is that it takes quite a long time to do the whole scan. For example, the scan whose results are shown in graphs 3.6 and 3.7 contains 594 points and took 4.5 hours to measure. But if we increased precision of the threshold scan the same scan could take up to 20 hours.

[21] In fact we take an average value from several strips to increase precision.

[22] Detector has two rows of strips where one row is bonded whereas the second row is not.

[23] Except for the metallic strip, because a light from the laser does not have enough energy to penetrate it.

[24] For example, a previous version of the silicon strip detector for ATLAS Upgrade, which was also tested at IPNP, did not satisfy this criterion because a loss of charge between the two strips was observed. Results of these laser tests where charge loss occurred are summarised in [12].

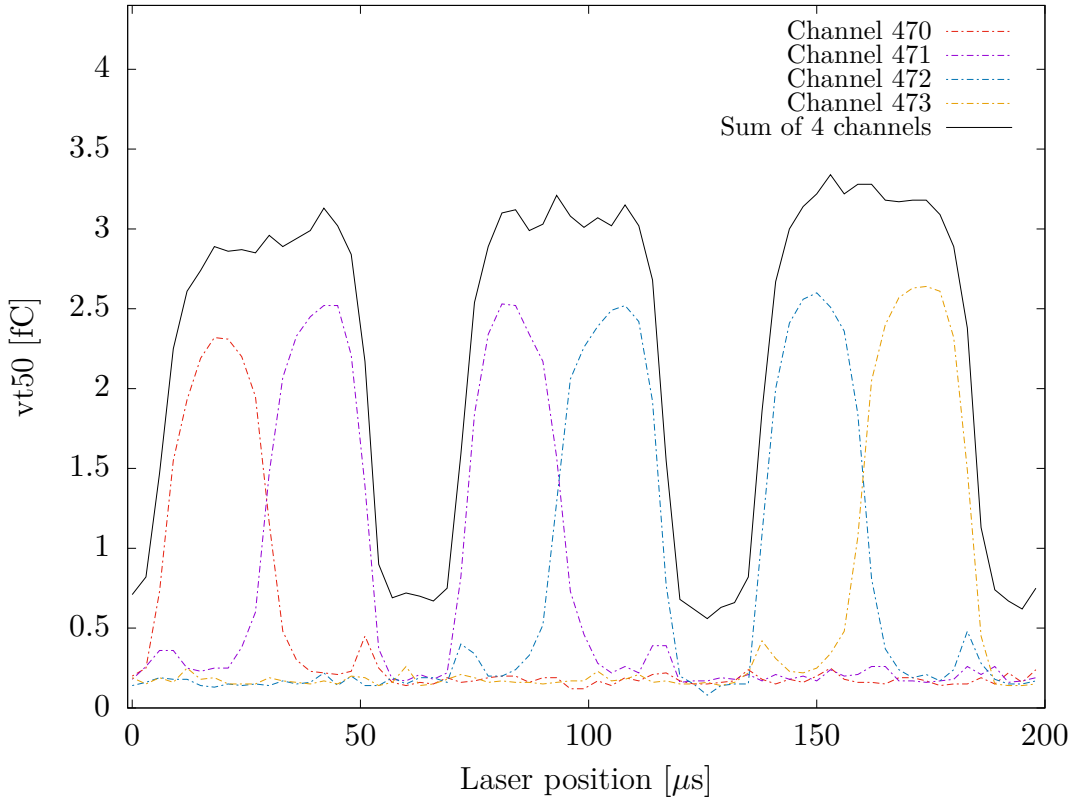

Graph 3.5: Interstrip scan. Dependence of detected signal on the laser position. Trigger delay was set to 40 μs. A typical relative uncertainty of measured data is 4% or less, but data points whose vt50 is close to 0 fC may have relative uncertainties up to 10%. The values of uncertainties were estimated by SCTDAQ.

In graphs 3.8 and 3.9 we can notice that for the laser position around 100 μm, there is a signal drop. This might be caused by an imperfection of the detector, or, more probably, by laser instability which will be later discussed in chapter 4.

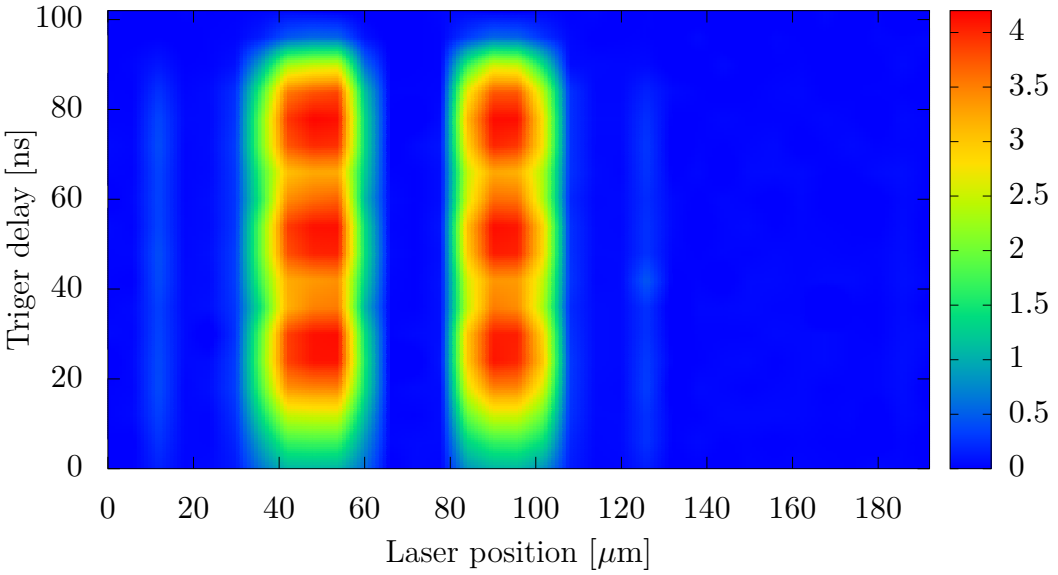

Graph 3.6: Heat map showing dependence of vt50 given in fC (represented on colour scale) on the laser position and trigger delay for one strip.

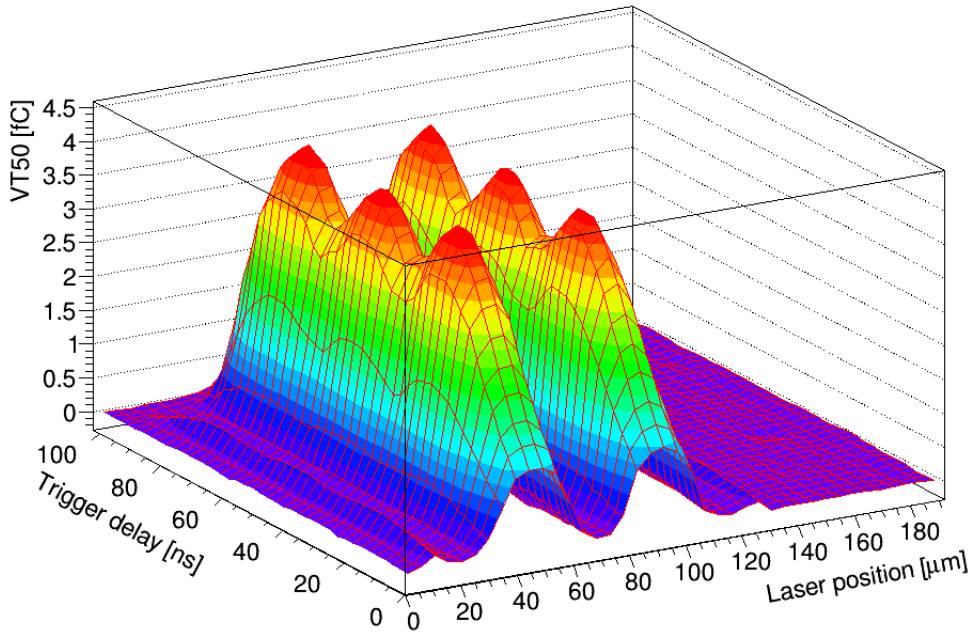

Graph 3.7: 3D visualisation of results shown on the heat map in graph 3.6.

Graphs 3.6 and 3.7 show response from only one strip. One may be also interested in what a response from the whole detector (sum of signal from all strips) would look like. Sum of signals from four neighbouring strips is depicted in graphs 3.8 and 3.9.

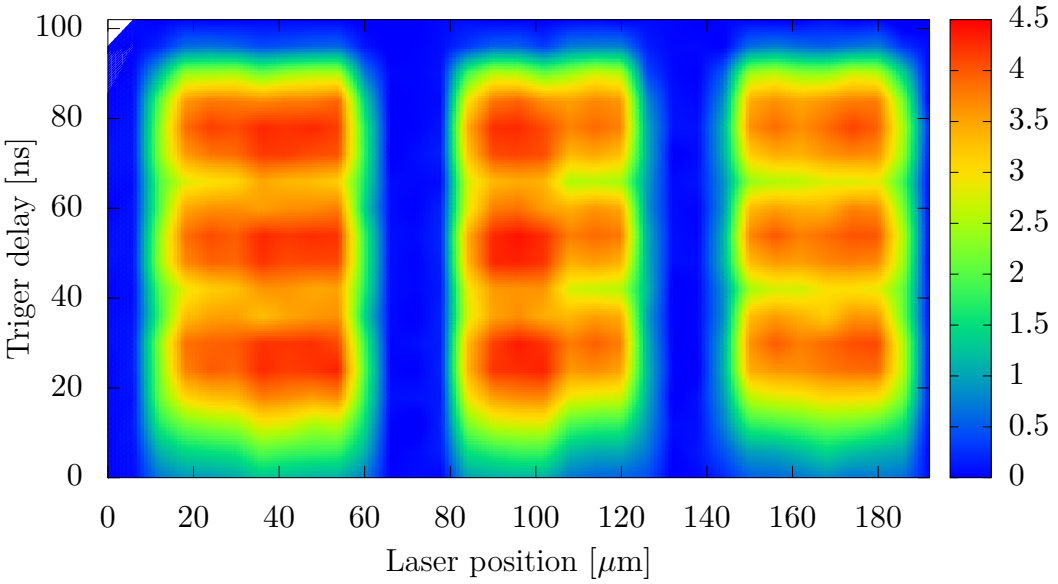

Graph 3.8: Heat map showing the dependence of the sum of signal from four neighbouring strips (represented on colour scale) on the laser position and trigger delay. Quantity on colour scale is the sum of vt50 in fC. It can be easily seen where the metallic electrodes (strips) are located. They are placed at positions where we get no signal from the detector, e.g. positions between 60 μm and 80 μm, or 130 μm and 150 μm.

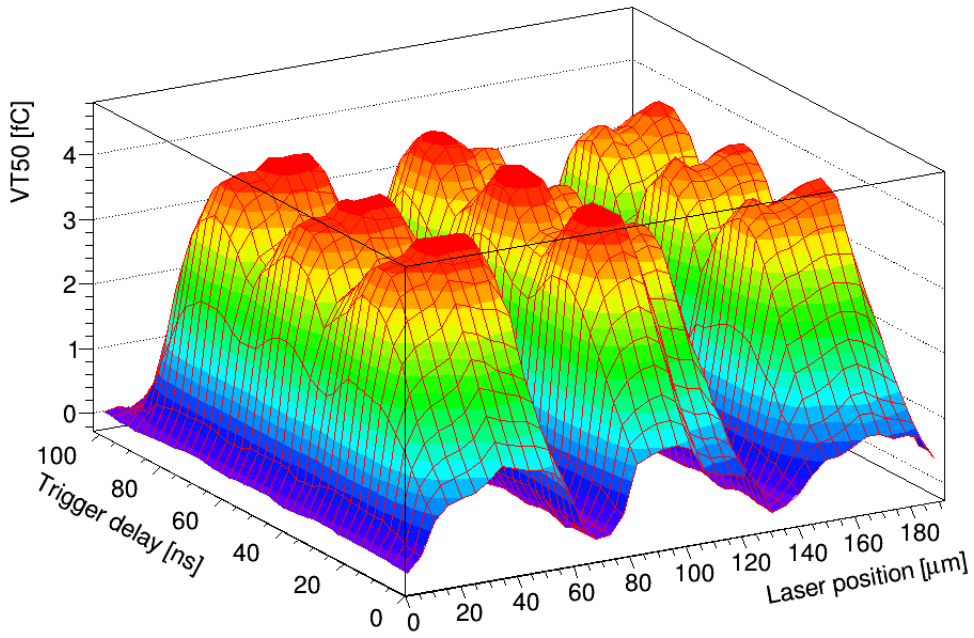

Graph 3.9: 3D visualisation of results shown on heat map in graph 3.8.

3.4 Macros used during testing

3.4.1 Measurement

It would be barely possible to do all the measurements above manually, because of the amount of measured values. For this reason, we wrote few C++ macros, using data analysis framework ROOT, to make these measurements easier. Because a lot of functions we needed was already written and were already succesfully used in the laboratories at IPNP we took the liberty of using some of these functions in our analysis. These were for example the functions for GPIB[25] communication with devices such as the pulse generator or functions for controlling the moving stages to which the laser was attached.

It turned out to be useful to use only one macro both for the one-dimensional measurements, such as for example the interstip scan, and the two-dimensional measurements. This is because we can use only one macro which is more flexible, as we can measure the whole two-dimensional dependence and then, by another macro used for graph plotting, select the desired section through the two-dimensional graph. This is beneficial because we can decide which sections are interesting for us whenever after measurement. Flowchart of the macro used for the measurement is shown in figure 3.6.

The macro is called `TrgDelay2D_ATLYS_OT.cpp`. Running it, to perform a measurement, requires setting several variables. They are:

`float Start`	Starting value of delay in [ns]
`float Stop`	Ending value of delay in [ns]
`float StepSize`	Size of step in trigger delay parameter in [ns]
`float VThr_start`	Initial value in threshold scan given in DAQ counts
`float VThr_stop`	Ending value in threshold scan given in DAQ counts
`float VThr_step`	Threshold scan step size given in DAQ counts
`int Ntrigs`	Number of triggers for each threshold
`int LTDirection`	Axis in which the laser should move[26]
`float LTStepSize`	Step size of laser shift in [mm]
`int LTSteps`	Number of laser shifts during measurement

The table containing values of variables used in measurements presented above is included in the attachments to the thesis as attachment 1. The table contains also additional pieces of information about values set on the pulse generator and about conditions in laboratory during measurement.

3.4.2 Graph plotting

It was mentioned that we measured two-dimensional dependencies and then used a macro for graph plotting. This is the second macro written as a part of this thesis. It is called `Plots_OT.cpp`. It can plot two-dimensional dependence of vt50 on trigger delay and laser position from one strip or from the whole detector,

[25] GPIB is an abbreviation which stands for General Purpose Interface Bus. This is an 8-bit, electrically parallel bus which is commonly used in instrumentation.

[26] 1 corresponds to x-axis, 2 corresponds to y-axis and 3 stands for z-axis.

which is the sum of signals from the individual strips. It is also capable of plotting sections through two-dimensional graph which are perpendicular to the time delay axis or laser position axis. Examples of these sections are graphs 3.1, 3.2, 3.3, 3.4 or 3.5. This macro also converts DAQ counts (internal units of analog-to-digital converter) to fC which are units that can be interpreted in more physical terms. Because the conversion is not straightforward, it will be described in greater detail in the following subsection.

3.4.3 Conversion from DAQ counts to fC

This conversion has two stages. First is the conversion from DAQ counts to millivolts where the conversion function is same for whole detector. The second stage depends on the strip number, because response of each strip is different. For this reason it is necessary to do module characterisation[27]. Because module characterisation was not subject of this thesis, we used already measured data for this purpose.

The conversion function from DAQ counts to mV is plotted in graph 3.10 with red marks. It can be seen that for a wide range of DAQ counts, the function behaves linearly. For this reason we fitted the data points by a linear function which is a sufficient approximation for signals which we get from the detector after illuminating it by laser.

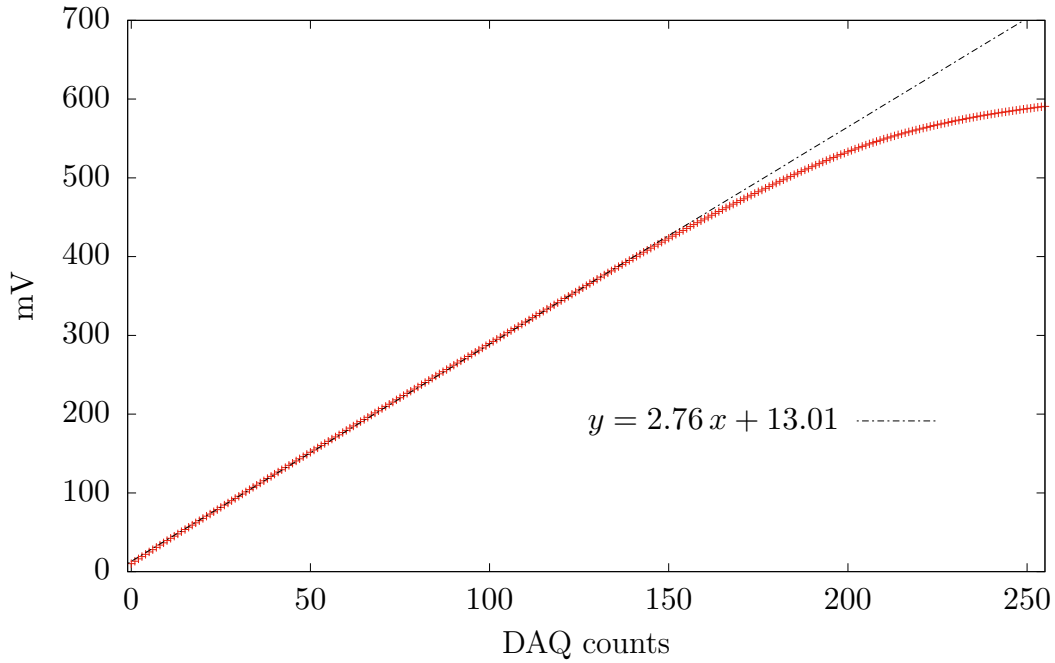

Graph 3.10: Conversion from DAQ counts to mV.

[27]Characterisation is done by an internal calibration pulse of given amplitude so that we know what the generated charge should be and we also know what we measure. By comparing this information for several pulses for each strip, we get the so called response curve which is in general a nonlinear function, but for small values of voltage it behaves linearly. So instead of measuring the whole response curve it is sometimes sufficient to measure the so called three point gain (3PG). It is the response curve for small values of voltage measured in three points fitted by linear function.

To be able to do the conversion from mV to fC, we need to know the response curve, or at least the 3PG, of each strip. Examples of such a response curve and 3PG curve of one strip were shown in graph 2.1.

Conversion from DAQ counts to fC is implemented as a function and used during graph plotting.

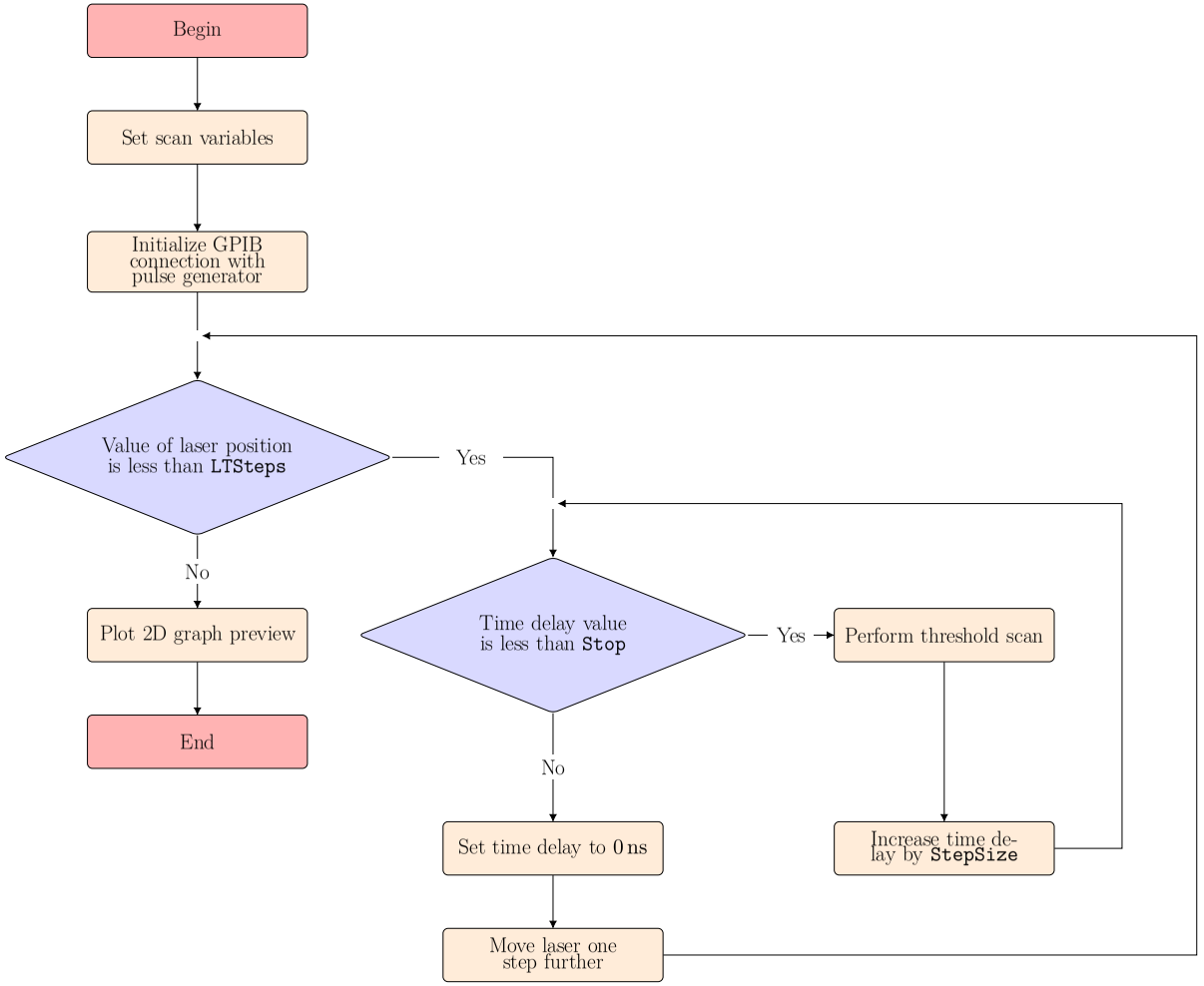

Figure 3.6: Flowchart of a macro `TrgDelay2D_ATLYS_OT.cpp` controlling two-dimensional laser scan.

4. Discussion

Results of the measurements and especially effects which might influence these results are discussed in this chapter. We would also like to point out some things which might be improved.

4.1 Discussion of results

First we measured dependence of signal from the detector on the trigger delay. We found that for certain delays signal drop can be observed. This is an unwanted effect which is caused by limitations of front-end electronics. In spite of this undesirable effect, we are able to roughly estimate, thanks to this measurement, the uncertainties of our results. Moreover, it provides us with the knowledge of the times, when the best response from the detector occurs.

Closely related to the previous measurement is the relation between the standard deviation σ and the trigger delay. It showed us that in comparison with the contributions from the front-end electronics of the detector and from the strips (these two are approximately equal), the largest source of errors is the laser. We also observed that the relative standard deviation increases when signal from the detector becomes weaker.

The third measurement we did was the measurement of the relation between the signal from the detector and laser position. If we compare our results with those listed in [12] we can say that we did not observe such a big charge loss between two strips. This is because the module we tested was different from the one which was inspected in [12]. So the results of our measurements appear to show that the issue with charge loss was eliminated on the current version of the detector.

Finally we measured two dimensional dependency of signal strength on trigger delay and laser position.

4.1.1 Effects influencing measurements

All measurements were affected by several unfavourable effects. Even though we tried eliminating them as much as possible we were not able to get rid of them completely.

The whole experimental setup was placed in a clean room, i.e. a room with low level of environmental pollutants. To avoid polluting the room, one has to wear a white cloak when inside. There is also a constant overpressure so that the outcoming air prevents the outside dust particles from contamining the room. Also, the interior of the room is kept within a given range of temperatures. The fact that the temperature can slightly vary in time[28] actually poses a problem: these temperature changes can slightly influence the power of the laser by causing thermal expansion of laser's resonant optical cavity, thereby bringing further uncertainty to our measurements.

[28]The room has its own half-an-hour-long cycle in which the temperature may change by up to 3 °C

Apart from the thermal changes there are probably some other effect causing instability of laser. For this reason we performed two independent measurements of laser stability with different laser settings, results of which are shown on graphs 4.1 and 4.2. In these measurements, we pointed laser at one spot on the detector and performed a series of threshold scans without changing any parameter. Even though the changes did not turn out to be too large, it still represents a severe problem.

We think that another effect influencing our measurements might be humidity. The effect of humidity on detection properties of detectors are known thanks to measurements from other laboratories.[13]

4.1.2 Room for improvements

There is still some room for improvements related to the reduction of laser instability. One possible solution of the problem is to use optical attenuator which can reduce laser's instability.

It was also mentioned that humidity can influence results of measurements. Currently it is not possible to control the level of humidity in the laboratory. Nevertheless, once we are able to control the level of humidity in our laboratory, future measurements of the effects of humidity on detectors would be highly appreciated.

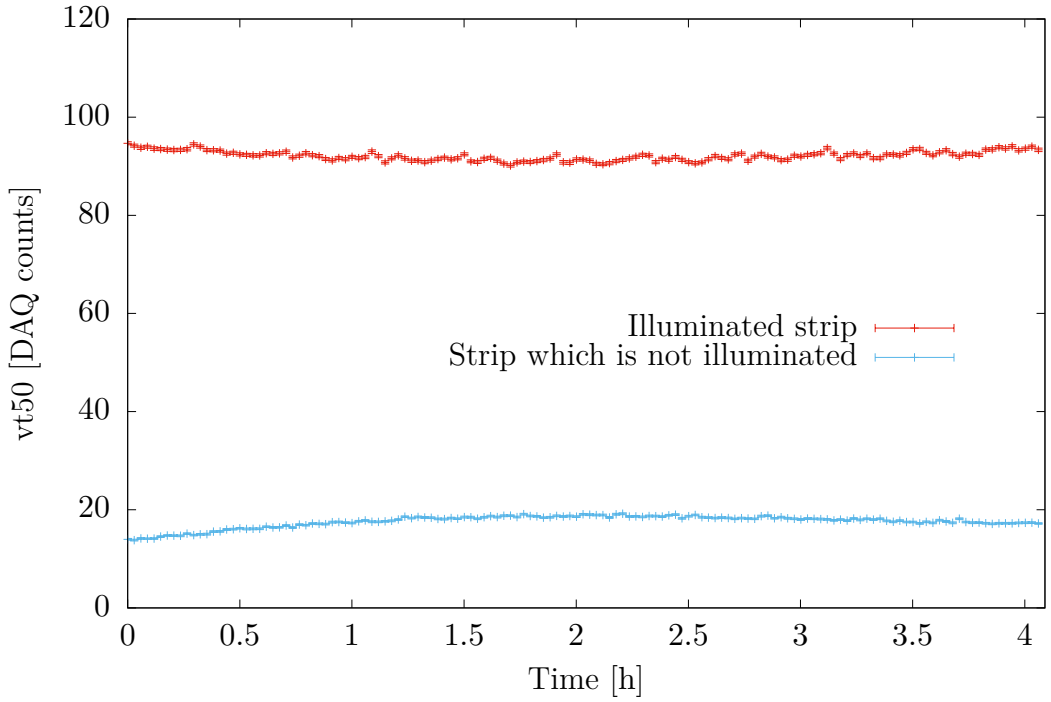

Graph 4.1: Signal from a strip illuminated by laser and from a strip which is not illuminated. It can be seen that the intensity of laser slightly varies in time.

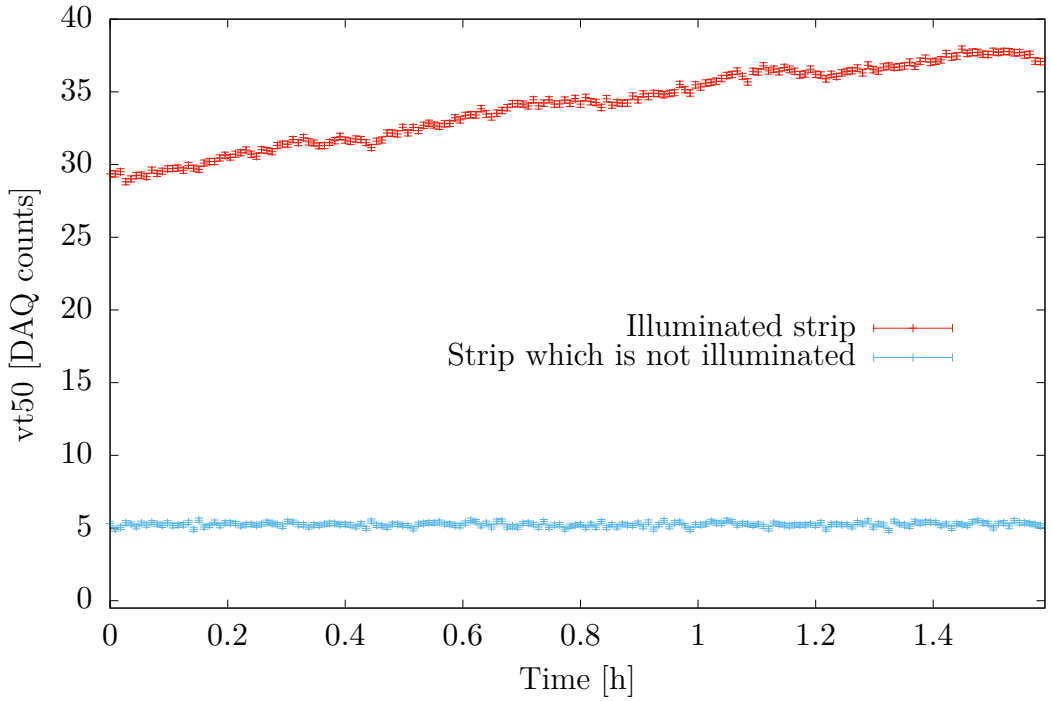

Graph 4.2: Signal from a strip illuminated by laser and from a strip which is not illuminated. It can be seen that the intensity of laser varies much more than in case of measurement presented on graph 4.1. Changes in intensity are significantly bigger than the error estimates.

Conclusion

In four chapters, this thesis offered the reader a number of insights into the problematics of laser testing of silicon strip detectors. The first two chapters were introductional. While the first chapter provided information about the planned changes to the ATLAS experiment at CERN, the second chapter explained the basic principles of silicon strip detectors and introduced some terms which were used later on. The main chapter was dedicated to experimental part and summarised all the tests done by the author of the thesis. Results of tests were discussed in the last chapter.

Work done within the thesis helped to refine the procedure of testing of the response from the detector as a function of trigger delay parameter and laser position. It also helped to automatize the analysis of measurements like data visualization, including conversion from DAQ counts to fC on new detectors and new versions of SCTDAQ. Additionally some effects influencing laser stability were identified. Moreover, the macros written within the thesis can be used during future work in the laboratories of IPNP. Finally, the measurements performed within the thesis contributed to certain extent to understanding the detection properties of newly produced pieces of silicon strip detectors which will be placed in the ATLAS Upgrade experiment.

Bibliography

[1] About the ATLAS Experiment | ATLAS Experiment at CERN. http://atlas.cern/discover/about, February 2016 (accessed March 1, 2017).

[2] The High-Luminosity LHC. http://home.cern/topics/high-luminosity-lhc, January 2017 (accessed March 2, 2017).

[3] ATLAS. http://atlas.cern/resources/multimedia/detector, April 2014 (accessed March 7, 2017).

[4] Inner Detector. http://atlas.cern/discover/detector/inner-detector, January 2017 (accessed March 2, 2017).

[5] The ATLAS Collaboration. ATLAS Phase-II Upgrade Scoping Document. https://cds.cern.ch/record/2055248/files/LHCC-G-166.pdf, September 2015 (accessed March 6, 2017).

[6] T. Flick. The Phase II ATLAS Pixel Upgrade: The Inner Tracker (ITk). *JINST*, 2016.

[7] Calorimeter. http://atlas.cern/discover/detector/calorimeter, September 2015 (accessed March 6, 2017).

[8] Pseudorapidity. https://en.wikipedia.org/wiki/Pseudorapidity, September 2016 (accessed March 7, 2017).

[9] Trigger and Data Acquisition System | ATLAS Experiment at CERN. http://atlas.cern/discover/detector/trigger-daq, January 2016 (accessed March 7, 2017).

[10] Atlas magnet system - information. http://atlas-magnet.web.cern.ch/atlas-magnet/info/, 2007 (accessed March 15, 2017).

[11] Z. Doležal. Polovodičové detektory v jaderné a subjaderné fyzice. http://www-ucjf.troja.mff.cuni.cz/dolezal/teach/semicon, 10 2016.

[12] Lucia Meszarosová. The ATLAS Inner Detector Upgrade. Master's thesis, Institute of Particle and Nuclear Physics, 2016.

[13] Kroll J., Mikeštíková M. et al. Long-Term Stability of ATLAS12 Main Sensors humidity dependence. 2016. ATLAS ITk Week conference entry.

List of Abbreviations

3PG	Three Point Gain
ATLAS	A Toroidal LHC Apparatu s
DAQ	Data acquisition
GPIB	General Purpose Interface Bus
HL-LHC	High- Luminosity Large Hadron Collider
ITk	Inner Tracker
IPNP	Institute of Particle and Nuclear Physics
LAr	Liquid Argon Calorimeter
LHC	Large Hadron Collider
MS	Muon Spectrometer
SCT	Semiconductor Tracker
TDAQ	Trigger and Data Acquisition System
TileCal	Tile Calorimeter
TRT	Transition Radiation Tracker

Attachments

Attachment 1

		Number of graph in which the results of the particular measurement are presented		
		3.1, 3.2, 3.3, 3.4	3.5	3.6, 3.7, 3.8, 3.9
Name of the variable in macro `TrgDelay2D_ATLYS_OT.cpp`	`float Start`	0	0	0
	`float Stop`	105	48	105
	`float StepSize`	3	8	6
	`float VThr_start`	0	0	0
	`float VThr_stop`	200	200	200
	`float VThr_step`	2	2	7
	`int Ntrigs`	60	60	70
	`int LTDirection`	2	2	2
	`float LTStepSize`	-0.006	-0.003	-0.006
	`int LTSteps`	9	66	33
Parameters on the pulse generator	High [V]	2.15	2.15	2.15
	Low [mV]	−40	−40	−40
	Width [ns]	10	10	10
	LeadE [ns]	5	5	5
Conditi-ons	Temperature [$^\circ C$]	24.6	23.8	24.6
	Pressure [hPa]	1021	1024	1023

The table containing parameters of measurements presented in the thesis. It contains the initial values of variables used for the measurements, values set on the pulse generator and conditions in the laboratory at the begining of measurements.